Solid-Phase Growth of Nanostructures from Amorphous Peptide Thin Film: Effect of Water Activity and Temperature

Jungki Ryu and Chan Beum Park*

Department of Materials Science and Engineering, Korea Advanced Institute of Science and Technology, 373-1 Guseong-dong, Yuseong-gu, Daejeon 305-701, Republic of Korea

Received January 3, 2008. Revised Manuscript Received March 28, 2008

We report the solid-phase self-assembly of nanostructures from amorphous thin film of aromatic peptides. The thickness of amorphous peptide film could be precisely controlled down to ~50 nm. Aligned nanostructures were grown from the film either by changing water activity in the vapor phase or by applying high thermal energy. The growth of peptide nanorods on solid substrate occurred via a water-vapor-mediated self-assembly process. We found that the peptide nanostructures could be "reversibly" dissociated and reassembled depending on the chemical composition of the vapor phase. We also observed that the phase transition of aromatic peptide occurs at extremely high temperatures above 100 °C, and the thermal aging of amorphous film resulted in the formation of peptide nanorods. In this work, the formation of peptide nanostructures from amorphous thin film was investigated by multiple analytical tools such as electron and atomic force microscopies, vibrational and diffraction spectroscopies, and differential scanning calorimetry. To the best of our knowledge, this is the first report for the self-assembly of peptides into nanostructures starting from amorphous thin film.

Introduction

The ability to build nanostructures from different starting materials allows the engineering of materials to have novel properties that cannot be obtained from bulk materials.[1] For example, one-dimensional (1D) nanostructured materials such as carbon nanotubes (CNTs), metal nanowires, and organic nanowires/nanotubes have attracted scientific and industrial interest because of their inherent novel properties and potential applications.[2–5] They were shown to be used for electrical or electrochemical detection of biological and chemical species in a highly sensitive manner because of the increased surface to volume ratio[2,5] while having higher mechanical strength than bulk-structured materials.[6,7] However, it is very difficult to fabricate nanostructures with different materials by conventional top-down lithographic techniques because they cannot cover the diversity of materials and make the formation of complex structures almost impossible. As an alternative to conventional lithographic methods, many research groups have used self-assembly approaches.[8] Self-assembly is a process in which small building blocks spontaneously form finely structured materials via weak interactions between them such as hydrophobic interactions, van der Waals interactions, and hydrogen bonds.[9,10] Contrary to conventional methods, rationally designed self-assembly process can be utilized in the formation of various nanostructures including complex 3D structures from different building block materials.[11]

Recently, research groups reported that it is also possible to fabricate one-dimensional nanostructures via self-assembly of peptides.[12–18] Because of their flexibility in functionality and molecular-recognition properties as well as the mild conditions required in the fabrication process,[17] studies on peptide-based nanostructures are rapidly increasing.[13–15] Among various peptide building blocks forming one-dimensional nanostructures, the simplest building blocks are aromatic dipeptides forming nanotubes.[16,19–21] These peptide nanotubes were applied for casting conduct-

* To whom correspondence should be addressed. Phone: 82-42-869-3340. Fax: 82-42-869-3310. E-mail: parkcb@kaist.ac.kr.

(1) Whitesides, G. M. *Small* **2005**, *1*, 172.
(2) Cui, Y.; Wei, Q.; Park, H.; Lieber, C. M. *Science* **2001**, *293*, 1289.
(3) Besteman, K.; Lee, J-O.; Wiertz, F. G. M.; Heering, H. A.; Dekker, C. *Nano Lett.* **2003**, *3*, 727.
(4) Javey, S. H.; Guo, J.; Wang, Q.; Lundstrom, M.; and Dai, H. *Nature* **2003**, *424*, 654.
(5) Virji, S.; Huang, J.; Kaner, R. B.; Weiller, B. H. *Nano Lett.* **2004**, *4*, 491.
(6) Yu, M-F.; Lourie, O.; Dyer, M. J.; Moloni, K.; Kelly, T. F.; and Ruoff, R. S. *Science* **2000**, *287*, 637.
(7) Kol, N.; Adler-Abramovich, L.; Barlam, D.; Shneck, R. Z.; Gazit, E.; Rousso, I. *Nano Lett.* **2005**, *5*, 1343.
(8) Whitesides, G. M.; Mathias, J. P.; Seto, C. T. *Science* **1991**, *254*, 1312.
(9) Whitesides, G. M.; Boncheva, M. *Proc. Natl. Acad. Sci. U.S.A.* **2002**, *99*, 4679.
(10) Whitesides, G. M.; Grzybowski, B. *Science* **2002**, *295*, 2418.
(11) Gracias, D. H.; Tien, J.; Breen, T. L.; Hsu, C.; Whitesides, G. M. *Science* **2000**, *289*, 1170.
(12) Ghadiri, M. R.; Granja, J. R.; Milligan, R. A.; McRee, D. E.; Khazanovich, N. *Nature* **1993**, *366*, 324.
(13) Hartgerink, J. D.; Beniash, E.; Stupp, S. I. *Science* **2001**, *294*, 1684.
(14) Vauthey, S.; Santoso, S.; Gong, H.; Watson, N.; Zhang, S. *Proc. Natl. Acad. Sci. U.S.A.* **2002**, *99*, 5355.
(15) Scheibel, T.; Parthasarathy, R.; Sawicki, G.; Lin, X-M.; Jaeger, H.; Lindquist, S. L. *Proc. Natl. Acad. Sci. U.S.A.* **2003**, *100*, 4527.
(16) Reches, M.; Gazit, E. *Science* **2003**, *300*, 625.
(17) Gao, X.; Matsui, H. *Adv. Mater.* **2005**, *17*, 2037.
(18) Hamley, I. *Angew. Chem., Int. Ed.* **2007**, *46*, 8128.
(19) Reches, M.; Gazit, E. *Phys. Biol.* **2006**, *3*, S10.
(20) Hendler, N.; Sidelman, N.; Reches, M.; Gazit, E.; Rosenberg, Y.; Ritcher, S. *Adv. Mater.* **2007**, *19*, 1485.
(21) Gupta, M.; Bagaria, A.; Mishra, A.; Mathur, P.; Basu, A.; Ramakumar, S.; Chauhan, V. S. *Adv. Mater.* **2007**, *19*, 858.

10.1021/cm800015p CCC: $40.75
Published on Web 06/06/2008

ing metal nanowires[16,22] and enhancing the sensitivity of electrochemical detection of biomolecules.[23]

In the present work, we first report the solid-phase growth of nanostructures from an amorphous thin film of aromatic peptides. The peptide thin film was prepared by placing a drop of diphenylalanine (FF) dissolved in 1,1,1,3,3,3-hexafluoro-2-propanol (HFIP) onto a solid surface in the complete absence of water vapor, followed by drying. According to scanning electron microscopy (SEM) and X-ray diffraction (XRD) analysis, the thin film was confirmed to be amorphous in nature. From this amorphous thin film as a starting point, we could grow nanostructures such as nanorods by applying proper amounts of water vapor or high thermal energy. While no structural changes were observed for films aged at a low water activity level (i.e., low humidity), aligned peptide nanorods were observed at a high water activity level (i.e., high humidity), which indicates that the peptide nanostructures were formed via a water-vapor-mediated, solid-phase self-assembly process. We also found that phase transition of diphenylalanine occurs at above 100 °C and thermal aging of amorphous film at high temperatures resulted in the formation of peptide nanorods. The solid-phase self-assembly processes were further analyzed by multiple tools such as UV/visible absorbance, Fourier-Transform infrared (FT-IR) spectroscopy, atomic force microscopy (AFM), thermogravimetric analysis (TGA), and differential scanning calorimetry (DSC).

Experimental Section

Materials. Diphenylalanine (FF) peptide in a lyophilized form was obtained from Bachem AG (Bubendorf, Switzerland). 1,1,1,3,3,3-Hexafluoro-2-propanol (HFIP), lithium chloride, potassium acetate, magnesium chloride, potassium carbonate, magnesium nitrate, copper chloride, sodium chloride, potassium chloride, and potassium nitrate were obtained from Sigma-Aldrich (St. Louis, MO). Deionized water (18.2 MΩ cm^{-1}), which was filtered by the Millipore Nanopure Water system, was used throughout the experiment.

Preparation of Amorphous Thin Film of Diphenylalanine. Fresh FF solution was prepared by dissolving as-received FF in HFIP at a concentration ranging from 1 to 100 mg/mL. To avoid the formation of any kind of aggregates, the FF solution was always prepared immediately prior to use. Transparent amorphous FF film was obtained by placing a drop of FF solution at a desired concentration onto substrate (10 mm × 10 mm) and drying in the absence of water vapor in a vacuum desiccator at room temperature.

Solid-Phase Growth of Nanostructures from the Amorphous Peptide Film. To examine the effect of water vapor on the growth of nanostructures from amorphous peptide film, we made a small chamber composed of a 60 mm Petri dish with two separated compartments. The amorphous peptide film and a fixed volume of saturated salt solution or pure water were loaded into each compartment and the Petri dish was sealed with parafilm and aluminum sealing film. Samples were then incubated at a constant temperature of 25 °C. Water vapor content or pressure inside the chamber was precisely controlled by using various kinds of saturated salt solutions.[24] Peptide nanostructures formed upon exposure to water vapor were dissociated into monomeric peptides by treating them with HFIP vapor only for several minutes. To take an electron micrograph, samples were dried in a vacuum desiccator. To grow nanostructures by applying thermal energy (thermal aging), amorphous peptide films were incubated at a constant temperature of 25, 50, 100, and 150 °C in the absence of water vapor.

Microscopies. Sample structures were analyzed by scanning electron microscope (SEM) and atomic force microscope (AFM). For electron microscopy, samples were coated with a thin film of platinum using SCD005 Pt-coater (Bal-Tec AG., Liechtenstein) and analyzed with an S-4800 field emission scanning electron microscope (Hitachi High-technologies CO., Japan) at an acceleration voltage ranging from 1 to 3 kV. Surface morphology of samples was studied using a Multimode AFM equipped with a Nanoscope IIID controller (Digital Instruments Inc., CA) in a tapping-mode. Representative images in each case were obtained by scanning different samples at four randomly selected spots over the entire film.

X-ray Diffraction (XRD). The structure of amorphous FF film and nanostructured-FF film formed on slide glass were analyzed with a Rigaku D/MAX-IIIC powder X-ray diffractometer (Rigaku, Co, Japan) equipped with a Ni filter under the following conditions: scan speed, 3°/min; Cu Kα radiation, $\lambda = 1.5418$ Å; scan range, 3−50°.

Fourier Transform Infrared (FT-IR) and UV/Visible Absorption Spectroscopy. Samples for FT-IR and UV/visible spectroscopy were prepared on Si wafer and quartz plate, respectively. A clean substrate without any peptide film was used as a reference. FT-IR spectra were obtained using a Hyperion 3000 spectrometer (Bruker Optics Inc., Germany) in an attenuated total reflection (ATR) mode and using a Ge single-crystal at a resolution of 4 cm^{-1}. UV/visible absorption spectra were obtained using a Biospec Mini (Shimadzu Co., Japan).

Thermal Analysis. Differential scanning calorimetry (DSC) and thermogravimetric analysis (TGA) of amorphous FF and nanostructured FF film were carried out using a DSC 204 F1 (NETZSCH, Germany) and thermogravimetric analyzer Q50 (TA Instrument, DE). Samples were heated from room temperature to 400 °C at a constant rate of 10 K/min in a nitrogen environment.

Results and Discussion

Solid-Phase Growth of Peptide Nanorods from Amorphous Thin Film. We observed the formation of transparent and flat peptide thin film without any surface features when diphenylalanine (FF) solution dissolved in HFIP was allowed to dry on a solid surface in the complete absence of water vapor (Figures 1A and 3A). XRD analysis shows that this transparent film is amorphous in nature (see Figure 5A). Because in many cases the initial thickness and uniformity of thin film could affect the final nanostructures after further treatments,[25] the ability to control the thickness of the thin film is critically needed. Here, the thickness of the amorphous film was precisely controlled by simply changing the FF concentration dissolved in HFIP. Figure 1B shows a linear relationship between the thickness of the thin film and the concentration of the solution on a solid substrate (10 mm × 10 mm). We could make a flat and uniform amorphous peptide thin film with a thickness ranging from 50 nm to 6 μm with FF solution with concentrations from 1 to 100 mg/mL.

(22) Carny, O.; Shalev, D.; Gazit, E. *Nano Lett.* **2006**, *6*, 1594.
(23) Yemini, M.; Reches, M.; Rishpon, J.; Gazit, E. *Nano Lett.* **2005**, *5*, 183.
(24) O'Brien, F. E. M. *J. Sci. Instrum.* **1948**, *25*, 73.
(25) Peng, J.; Xuan, Y.; Wang, H.; Yang, Y.; Li, b.; Han, Y. *J. Chem. Phys.* **2004**, *120*, 11163.

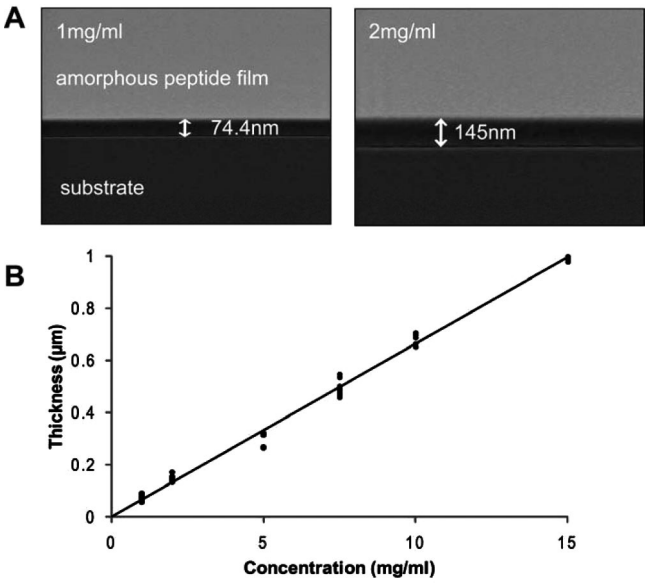

Figure 1. Formation of amorphous diphenylalanine (FF) thin film. The peptide film was formed by placing a 10 μL drop of FF solution in HFIP on substrate (10 mm × 10 mm) and drying in the absence of water vapor. (A) Side-view images of amorphous FF film formed on a substrate. The FF films were formed with a 10 μl drop of 1 mg/ml (left) and 2 mg/ml (right) FF solution in HFIP. (B) Graph showing the linear relationship between the film thickness and the concentration of FF solution used.

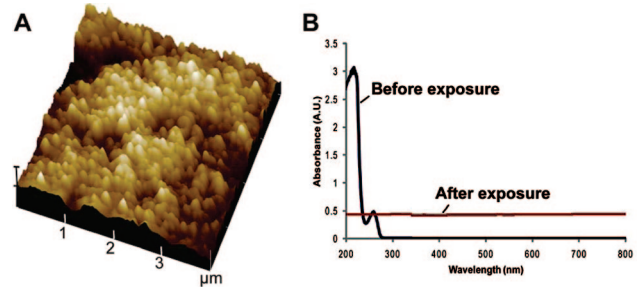

Figure 2. Effect of water vapor on the formation of peptide nanostructures. (A) Surface morphology of FF film was scanned by a tapping-mode AFM. rms values of the FF film before and after vapor treatment were 0.35 ± 0.01 and 24.11 ± 5.56 nm, respectively. (B) UV/visible absorption spectra of the FF film before (blue line) and after (red line) water vapor treatment.

Upon exposure of the amorphous film to saturated water vapor in a wet chamber, we could observe the growth of peptide nanorods on the film surface. After water-vapor exposure for 1 h at 25 °C, the root-mean-square roughness of amorphous film increased from 0.35 ± 0.01 nm to 24.11 ± 5.56 nm according to AFM analysis (Figure 2A). Cross-sectional analysis of amorphous films in the absence or presence of water vapor also clearly indicated that the morphological changes occurred during the incubation (data not shown). When we investigated the peptide thin film using SEM, we found short cylindrical objects that were formed on the film surface in the initial stage of water vapor treatment (Figure 3B). The average diameters of these objects, measured by SEM and AFM, were found to be 73.68 ± 11.65 nm and 93.40 ± 21.89 nm, respectively (sample size, $n = 50$). If we consider the effect of conductive coating for SEM and lateral broadening for AFM, the actual size of these spherical objects should be less than 80 nm. In addition, the UV/visible absorbance spectrum of the film significantly changed after the water-vapor exposure (Figure 2B). The amorphous film before the exposure presented no absorption peak in the visible region (300−900 nm) and two absorption peaks at 218nm and 258nm in the near UV region. This may result from $\pi-\pi^*$ electronic transition of aromatic ring in diphenylalanine.[26] After water-vapor treatment, the amorphous film exhibited a uniform absorbance of about 0.5 magnitude over the entire region. The water vapor should induce the change in the absorbance of the peptide film through an increased light scattering by the formation of discrete nanostructures on the film. Further aging of the amorphous film under saturated water vapor pressure for 24 h resulted in the film's being composed of well-aligned peptide nanorods (Figure 3C). The resultant film consisted of many domains showing different orientation of nanostructures and, in a single domain, all peptide nanostructures run parallel to each other (data not shown). Further incubation of peptide nanostructures under saturated HFIP vapor condition led to the dissociation of peptide nanostructures into amorphous FF film. The "reversible" self-assembly process was easily detected even with the naked eye since the nanorod film was translucent or opaque because of the scattering of visible light, whereas the amorphous film was transparent.

Influence of Water Activity on Solid-Phase Growth of Peptide Nanorods. We further investigated the effect of water vapor content (i.e., humidity) on the solid-phase growth of peptide nanostructures. A precise control of humidity was achieved by loading different kinds of saturated salt solution in a chamber. It is well-known that ionic salts dissolved in water lower the water activity, a_w, and that the water activity of saturated salt solution depends on the nature of each salt.[24] Because the relative humidity (RH) inside the chamber is proportional to the water activity of a salt solution (RH = $a_w \times 100\%$), we were able to observe the effect of water vapor on the self-assembly of aromatic peptide more systematically. Here we used ten different kinds of saturated salt solutions, which covered the full range of water activity from zero to one (Figure 4). While no structural change was observed at less than 50% RH (i.e., $a_w < 0.5$) even after aging for a week, peptide nanorods were formed at above 90% RH after 24 h of incubation. In between these two regimes, we could observe only small spherical aggregates (average diameter: 81.31 ± 15.25 nm, sample size $n = 50$) on surface, which resembled surface features formed in the initial stage of saturated water vapor exposure (Figure 3B). Once the nanostructured film was developed at the high water humidity, the nanostructures did not change with further incubation under lower humidity condition.

On the basis of our results, we propose that surface nucleation and mass-transport limitation may lead to the formation of well-aligned peptide nanostructures from amorphous thin film (Figure 3). We could easily observe nucleus-like objects on the sample surface with SEM or AFM at the initial stage of hydration (within 30 min). Because the water-vapor-mediated self-assembly is basically a solid-phase process, mass transport may be limited to a short time range. We speculate that the limitation of mass transport may lead

(26) Pavia, D. L.; Lampman, G. M.; Kriz, G. S. *Introduction to Spectroscopy*, 3rd ed.; Thomson Learning: Orlando, 2001.

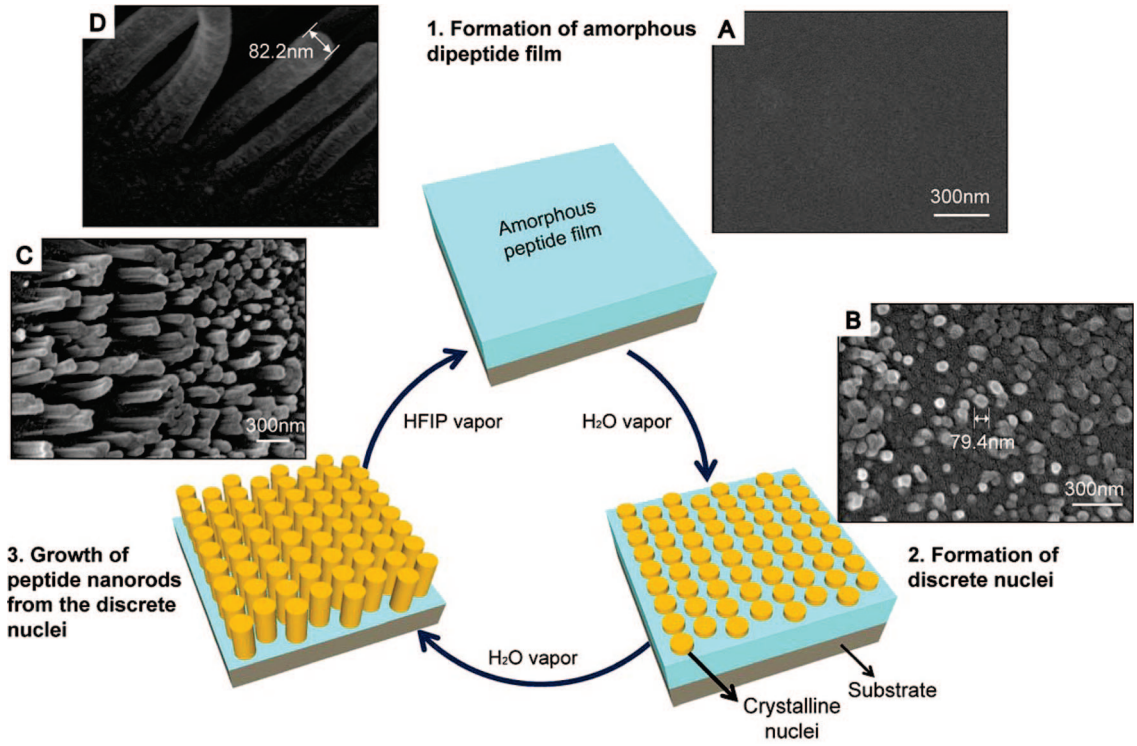

Figure 3. Electron micrograph and proposed hypothesis showing the effect of water vapor on the formation of ordered peptide nanostructures on a solid surface, self-assembled from diphenylalanine. (A) Amorphous FF film was formed by placing a drop of FF solution in HFIP on substrate and drying it in the absence of water vapor. (B) Discrete nuclei formed on the surface with brief exposure (ca. 30 min) to water vapor. (C, D) Peptide nanorods grown from the nuclei by further exposure to water vapor.

to the ordered growth of peptide nanostructures from the discrete nuclei that were formed by supersaturation of peptides upon the hydration of amorphous thin film. Our hypothesis is further supported by recent reports about the formation of polysiloxane nanofibers and the ordering of block copolymers during solvent-vapor aging.[25,27–29] In a conventional method for the preparation of flat and uniform organosilane thin film, water was excluded and only a trace amount of water remained in order to prevent the formation of large aggregates observed in the presence of excess water. Rollings and her colleagues reported a two-step process for the fabrication of polysiloxane nanofibers through surface initiated, vapor-phase polymerization of organotrichlorosilanes.[27] It is also well-known that block copolymer, which is one of the most widely studied self-assembling systems, could self-assemble into ordered nanostructures by solvent-vapor-assisted self-assembly in a so-called solvent-aging process. Disordered block copolymers could form ordered periodic nanostructures by enhancing their chain mobility with increased temperature above the glass transition point.[30] More recently, this ordering of block copolymers could be accomplished under solvent-vapor-assisted conditions.[25,28,29]

Structural Analysis of Peptide Nanorods on Solid Surface by XRD and FT-IR. In order to investigate structural characteristics of our samples, we carried out

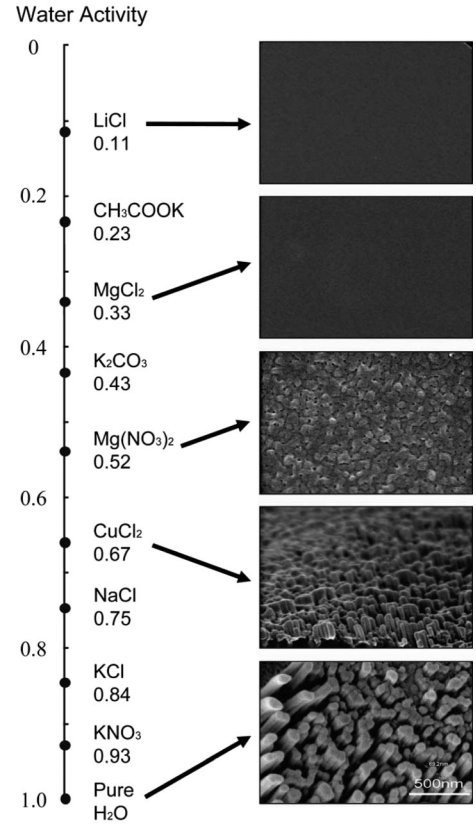

Figure 4. Effect of water activity on the morphology of self-assembled nanostructures from amorphous FF peptides. Amorphous peptide film was prepared with a 10 μL drop of 50 mg/mL FF solution and amorphous peptide film was then aged in a partitioned chamber for 24 h. Water-vapor content in the atmosphere inside the chamber was varied with different kinds of saturated salt solutions.

(27) Rollings, D-A.; Tsoi, S.; Sit, J. C.; Veinot, J. G. C. *Langmuir* **2007**, *23*, 5275.
(28) Kim, S. H.; Misner, M. J.; Russell, T. P. *Adv. Mater.* **2004**, *16*, 2119.
(29) Fukunaga, K.; Elbs, H.; Magerle, R.; Krausch, G. *Macromolecules* **2000**, *33*, 947.
(30) Park, M.; Harrison, C.; Chaikin, P. M.; Register, R. A.; Adamson, D. H. *Science* **1997**, *276*, 1401.

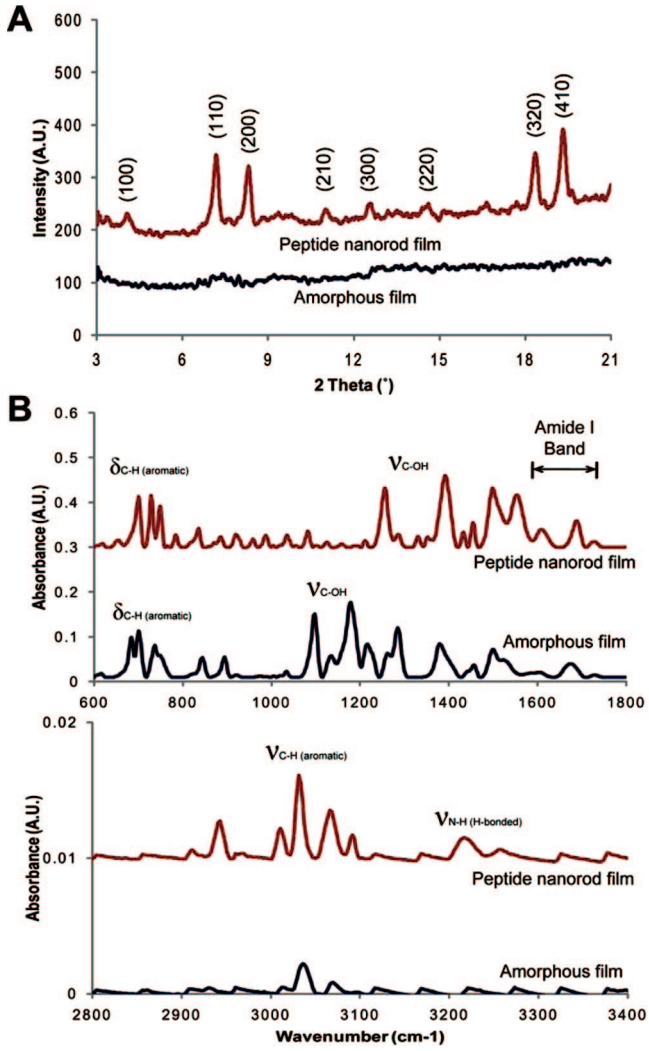

Figure 5. Results of X-ray diffraction and FT-IR spectrometry for peptide nanostructures formed on a solid surface. (A) X-ray powder diffractograms and (B) FT-IR spectra of samples dried in the absence or presence of water vapor are shown.

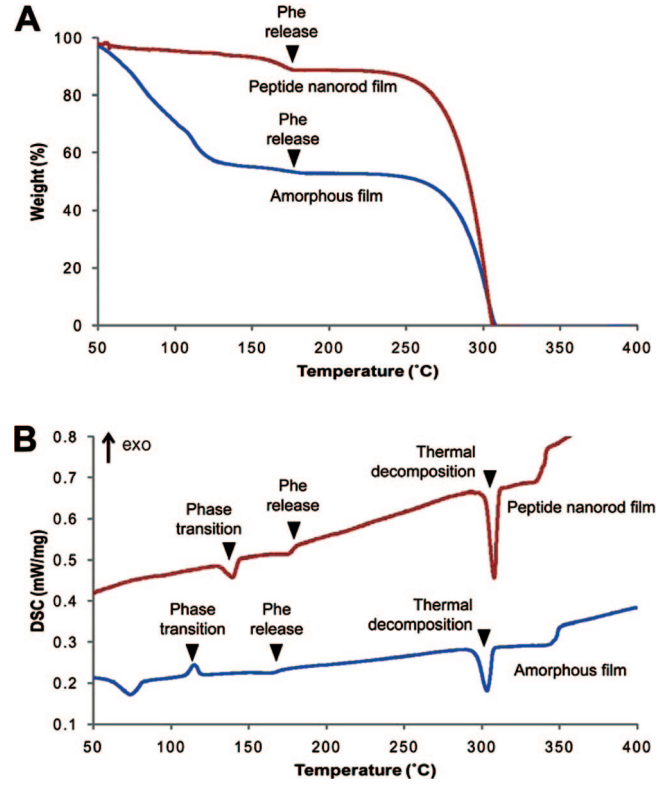

Figure 6. Thermal analysis of amorphous FF film before and after exposure to water vapor. Amorphous and nanorod films were characterized by (A) DSC and (B) TGA.

powder XRD and FT-IR analyses. Figure 5A shows the results of XRD obtained from amorphous film and nanorod film, respectively. Although the amorphous film of FF presents no diffraction peak, nanorod film exhibits several characteristic diffraction peaks. It is noteworthy that the powder diffraction pattern of the peptide nanorod film was very similar to the previously reported diffraction pattern of diphenylalanine nanotubes.[31,32] FT-IR analysis also confirms a distinct difference between spectra obtained from amorphous FF film and nanorod FF film (Figure 5B). FT-IR spectrum for nanorod FF film shows a shift of peaks from those for amorphous FF film with much stronger absorption intensity over almost the entire region. C−OH (on −COOH group) peaks located at 1097 and 1198 cm^{-1} shifted to 1255 and 1390 cm^{-1} after exposure to water vapor, respectively (about a 25% shift). In the case of C−H peaks on the aromatic ring at around 600−900 cm^{-1}, a shift of less than about 10% was observed. In addition, nanorods FF film exhibited new peaks at 1608 and 1687 cm^{-1} in the amide I band region, which can be assigned to β-sheet structure.[21] Previously, Gazit and Gorbitz independently suggested that $\pi-\pi$ interaction between aromatic rings and the formation of hydrogen bonding between water and peptide molecules may lead to the formation of aromatic peptide nanotubes.[32–34] Previous studies show that the formation of moderate and weak (including $\pi-\pi$ interaction) hydrogen bonds shifts IR vibrational peaks about 10−25% and less than 10%, respectively.[35,36] We could also observe a new IR peak at around 3200−3300 cm^{-1} in the present work. This new peak can be assigned to hydrogen-bonded N−H stretching frequency.[12] Thus, both XRD analysis and FT-IR spectra support the growth of peptide nanostructures by the formation of hydrogen bond upon exposure to water vapor.

Thermal Analysis of Amorphous and Nanorod Thin Film. Thermal properties of amorphous and nanorod thin films prepared by the water-vapor mediated self-assembly process were analyzed by TGA and DSC. According to TGA thermograms (Figure 6A), a slight weight decrease at near 175 °C was observed for both amorphous and nanorod film. Recently, Sedman and her colleagues reported that phenylalanine was released from diphenylalanine nanotubes when they were heated up to 200 °C.[37] The weight decrease of the peptide film at near 175 °C in the present work is also

(31) Reches, M.; Gazit, E. *Nat. Nanotechnol.* **2006**, *1*, 195.
(32) Gorbitz, C. H. *Chem Commum.* **2006**, 2332.
(33) Gorbitz, C. H. *Chem.—Eur. J.* **2001**, *7*, 5153.
(34) Gilead, S.; Gazit, E. *Supramol. Chem.* **2005**, *17*, 87.
(35) Jeffrey, G. A. *An Introduction to Hydrogen Bonding*; Oxford University Press: New York, 1997.
(36) Marechal, Y. *The Hydrogen Bond and the Water Molecule*; Elsevier Science: Oxford, U.K., 2006.
(37) Sedman, V. L.; Adler-Abramovich, L.; Allen, S.; Gazit, E.; Tendler, S. J. B. *J. Am. Chem. Soc.* **2006**, *128*, 6903.

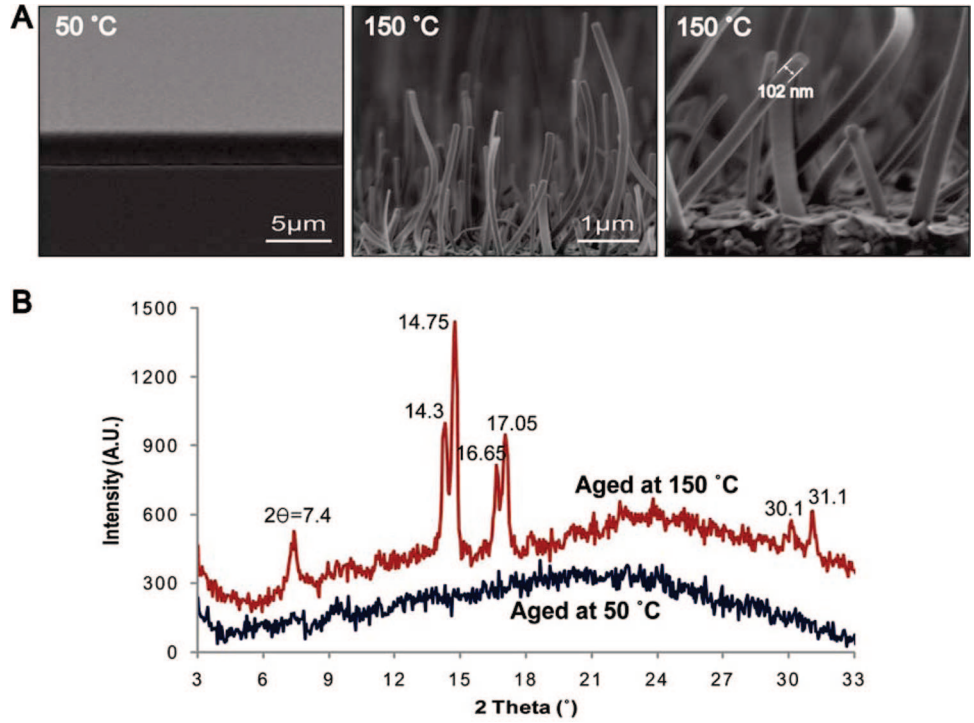

Figure 7. Formation of nanostructures from amorphous peptide film by thermal aging. Amorphous peptide films were thermally aged without water vapor at a temperature of 50 and 150 °C for 20 h. (A) Electron micrographs showing the effect of temperature on the growth of peptide nanostructure from amorphous peptide film in the absence of water vapor. (B) Powder X-ray diffractograms for peptide film aged at 50 °C (blue line) and 150 °C (red line) for 20 h.

thought to result from the release of phenylalanine, which was described by Sedman et al. The thermal decomposition of both peptide films was completed at 308 °C. Contrary to the nanorod film, amorphous FF film showed a rapid loss in weight of about 45% from around 60 to 100 °C, which can be attributed to the evaporation of residual HFIP in the amorphous film. DSC analysis of both films presented two endothermic peaks: one at around 175 °C corresponding to thermal release of phenylalanine from diphenylalanine and another one at around 308 °C corresponding to thermal decomposition of the films (Figure 6B). In the case of amorphous peptide film, there existed an endothermic peak centered at 73.5 °C corresponding to the evaporation of HFIP. In addition to those peaks, DSC thermograms for amorphous and nanorod film presented an exothermic peak at 115 °C and an endothermic peak at 139.3 °C, respectively. We speculate that these peaks arose from a phase-transition of FF film since there was negligible weight decrease in the TGA thermogram near these temperatures.

Growth of Nanostructures by Thermal Aging of Amorphous Thin Film. Interestingly, thermal aging of the amorphous peptide film at high temperatures resulted in the formation of rodlike nanostructures on the solid surface (Figure 7). Initially, we incubated the amorphous film in the absence of water vapor at a constant temperature to assign the peaks in the DSC thermogram. After thermal aging of the film for 20 h, we analyzed each sample by SEM. When the film was aged at a low temperature of less than 50 °C, no structural change was identified, but rodlike nanostructures were formed on the film surface when it was aged at higher temperatures at above 100 °C (Figure 7A). We could assign the exothermic peak at 115 °C for amorphous peptide film and the endothermic peak at 139.3 °C to the phase transition into the nanofibrillar phase. Note that the discrepancy in the temperature of phase transition between the DSC analysis and the thermal aging experiment should originate from different experimental conditions; samples were aged at a constant temperature during the thermal aging experiment, whereas samples heated gradually from room temperature to 400 °C at a constant rate of 10 K/min during the DSC analysis. Phase transition behavior of the amorphous film was also confirmed by powder XRD analysis (Figure 7B). Although the films aged at 25 and 50 °C remained amorphous, the film aged at 150 °C exhibited characteristic diffraction peaks. In addition, the diffraction pattern of thermally aged peptide film was significantly different from that of solvent-aged peptide film (Figures 7B and 5A). From the results of TGA, DSC, SEM, and XRD analysis, we could confirm that the formation of peptide nanorods induced by thermal aging was a result of the phase transition of diphenylalanine. The formation of ordered nanostructures by aromatic peptide at such high temperature as 150 °C is surprising from a biological point of view, considering that the structures of most peptides or proteins start to denature even at 50 °C, except for those from thermophilic microorganisms.[38] Further studies are required to understand the underlying mechanism of diphenylalanine self-assembly at such high temperature.

Conclusion

In summary, we have shown the self-assembly of a small peptide into nanostructures such as nanorods from solid-

(38) Meersman, F.; Heremans, K. *Biochemistry* **2003**, *42*, 14234.

phase amorphous thin film. The inherent mass transport limitation of the solid-phase process resulted in the formation of well-aligned peptide nanostructures from amorphous thin film in water-vapor-mediated self-assembly mechanism. We could reversibly dissociate and reassemble peptide nanorods by controlling the water activity in the atmosphere. In addition, we found that at extremely high temperatures ranging from 100 to 150 °C, peptide nanorods form from the amorphous thin film. Our peptide nanostructures are expected to be further used as a template for nanostructured materials on various substrates from amorphous (e.g., glass) to crystalline (e.g., silicon wafer). We believe that the solid-phase growth of peptide nanostructure from an amorphous thin film may provide a new approach for peptide-based nanofabrication because positioning and dispersion problems can be readily eliminated or minimized compared to conventional solution-phase methods.

Acknowledgment. This study was supported by the Korea Research Foundation (Grant KRF-2006-D00078). The authors thank the National NanoFab Center (NNFC) in Korea for technical support in the characterization of peptide nanostructures.

CM800015P